How Does Policy Stringency Affect the Spread of COVID-19 Pandemic? A Country Level Study

Yicong Li, Calvin Chan, Yang Li*, Ercan Engin Kuruoglu*
Tsinghua-Berkeley Shenzhen Institute
Tsinghua University
Shenzhen, China
{li-yc19, chanc10}@mails.tsinghua.edu.cn, {yangli, kuruoglu}@sz.tsinghua.edu.cn

***Abstract*—Starting the end of 2019, COVID-19 has developed into a global pandemic demonstrating a wide range of different dynamics temporally and spatially due to different strategies taken by different countries over time. It is vital to systematically investigate how policies affect the spread of COVID-19 pandemic. In this paper, we propose a statistical signal processing framework to evaluate the effectiveness of containment and closure policy on the epidemic dynamics and provide case studies on four countries: United States, United Kingdom, Italy, and Turkey. Particularly, we propose to use unscented Kalman filter to estimate the time-varying reproduction number of each country. Then by using causality analysis and change point detection, we show that the time-series of policy stringency Granger-causes the time-series of reproduction number in the cases of United States and Italy with 3 to 13 and 17 days delay respectively.**

***Index Terms*—epidemic models, unscented Kalman filter, Granger causality test, change point detection**

I. Introduction

First identified in Wuhan, China in December 2019, the coronavirus disease (COVID-19) has led to a global pandemic. Causing more than 2.4 million deaths over the past 14 months worldwide, the pandemic has and will continue to cause unprecedented economic recession globally in the near future [1]. Since the start of the COVID-19 outbreak, governments around the globe have implemented a wide range of containment policies in response to it, such as social distancing, curfews, school and business closures with various stringency [2]. Despite the success of controlling the spread of virus in some countries, the global pandemic is still far from being under control. In order to help government agencies to improve their policy decision making, it is important to evaluate the effect of the past policies on controlling the spread of the disease in a quantitative way, i.e. whether the implementation or lifting of policies accounts for a causal factor of changes in the epidemic dynamics and how long it takes for policy changes to take into effect.

In this paper, we study the problem of evaluating the effect of containment and closure policy stringency on epidemic spread for a given country. This problem involves three challenging components: 1) accurate tracking of the dynamics of COVID-19 pandemic spread from available data, 2) identifying the causal effect of policy stringency changes, and 3) evaluating the policy effectiveness as well as the response time. Modelling the spread of epidemics has been studied in the literature starting with the work of Kermack and McKendrick [3]. Many widely used compartmental models have been developed, such as SIR and SEIR [4], [5]. There are more advanced models like SEIRD [6] and SEIAHRD [7] that also consider an additional Deceased state in comparison with SEIR, however this may introduce additional noise due to the data collection delay for the deceased. More recently, tracking-based algorithms are also used to model the pandemic spread, e.g. in [8], Kalman filter (KF) is used to make short-term prediction of daily new cases in Wuhan, China. The model can forecast the daily cases three days in advance which benefits resource allocation. In [9], extended Kalman filter (EKF) is used to track the number of positive, recovered and deceased cases. Meanwhile, the problem regarding what policy would be most effective in controlling the COVID-19 pandemic is also explored by researchers with either deterministic model-based or data-driven approach. [10] develops a modified SEIR model with extra parameters for social distancing, age stratification, and lockdown to evaluate the effectiveness of vertical confinement and release in Brazil. [11] also measures the impact of non-pharmaceutical interventions (NPIs) on the spread of COVID-19 by introducing a modified SEIR model and tracks model parameters with ensemble adjustment Kalman filter. The impact of different combinations of intervention policies are compared in [12] using a stochastic age-structured transmission model. It concludes that intensive interventions with lockdown periods is needed in United Kingdom. As for data-driven approaches, machine learning techniques such as random forests are utilized by [13] to assess the influence of government interventions on mitigating COVID-19 and [14] leverages a Bayesian hierarchical model to link NPIs implementation dates to national case and death counts for effectiveness estimation.

However, due to the complexity of the time-varying dynamics under multiple influences, to the best of our knowledge, there hasn't been a study that retrospectively investigate how containment and closure policy stringency affect the pandemic spread. To this end, we develop an algorithmic framework (shown in Fig. 1) to track the spread of COVID-19 pandemic and analyze the causal effect between policy stringency and pandemic spread. We first propose using unscented Kalman

The first two authors contributed equally to this work. Asterisks indicate corresponding authors.

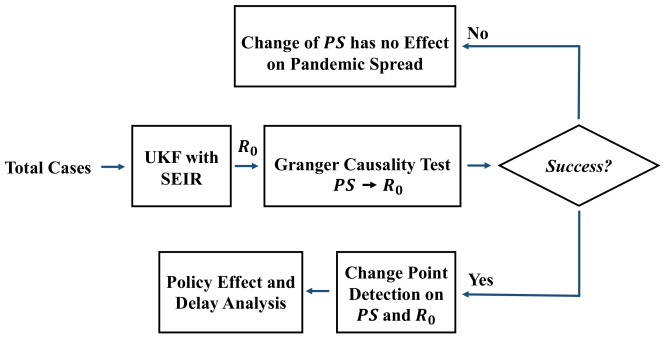

Fig. 1. Propsed Framework. PS: Policy Stringency. R_0: Reproduction Number.

filter (UKF) [15] to track and estimate the time-varying reproduction number R_0. UKF uses a deterministic sampling approach that has advantages of more accurate state prediction, easier implementation, and better computational efficiency compared to aforementioned EKF-based methods. R_0, defined as the number of people that one infected person will pass on a virus to on average, is widely used in COVID-19 studies representing the trend of the pandemic. Granger causality test [16] is then conducted on four countries to investigate the relationship between reproduction number and stringency of containment and closure policy. Furthermore, change point detection is performed to identify the response delay of R_0 to the change of containment and closure policy stringency.

II. Methods

A. Susceptible-Exposed-Infectious-Recovered (SEIR) Model

Fig. 2 illustrates the structure of SEIR model. *Susceptible state* (S) represents the number of individuals who are able to contract the disease. *Exposed state* (E) represents the number of individuals who have been infected but are not yet infectious. *Infectious state* (I) represents the number of individuals who are capable of transmitting the disease. *Recovered state* (R) represents the number of individuals who have become immune. *Transmission rate* ($\beta = \beta_0 t$) is the average number of contacts per person at each time step (t), multiplied by the probability of disease transmission in a contact (β_0). Reciprocal of incubation rate ($1/\alpha$) is the mean latent period with "days" as unit. In this paper, α is fixed at $1/5.2$ according to [17]. Reciprocal of recovery rate ($1/\gamma$) is the mean infectious period also with "days" as unit. And reproduction number $R_0 = \beta/\gamma$. Normally, larger value of R_0 means harder control of pandemic. Furthermore, SEIR model has the following assumptions:

1) Population N of a country is fully partitioned into susceptible, exposed, infectious, and recovered state, and is treated as a constant, i.e., $N = S + E + I + R$.
2) The transmission, incubation, and recovery rate are the same for individuals.
3) People contact each other randomly.

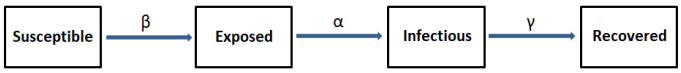

Fig. 2. SEIR Model

With the above assumptions, SEIR model can be described by ordinary differential equations as follows:

$$\begin{aligned} dS/dt &= -\beta IS/N \quad dE/dt = \beta IS/N - \alpha E \\ dI/dt &= \alpha E - \gamma I \quad dR/dt = \gamma I \end{aligned} \tag{1}$$

B. Unscented Kalman Filtering with SEIR Model

Unscented Kalman filter (UKF) is used to track the states S, E, I, R, and parameters β, γ. This involves a discrete-time nonlinear dynamic system,

$$X_t = f(X_{t-1}) + v_t \tag{2}$$

$$Y_t = h(X_t) + n_t \tag{3}$$

where $X_t = [S_t, E_t, I_t, R_t, \beta_t, \gamma_t]$ represents the unobserved states of the system at time step t, and Y_t is the observed measurement, i.e., total cases at time step t. The process noise v_t drives the dynamic system, and the measurement noise is given by n_t. In our case, the system dynamic model f is the SEIR model as shown in (1). And $h = E + I + R$ is the measurement function. UKF approximates the probability distribution of an unobserved state by selecting a minimal set of sample points such that their mean and covariance are the same as the true probability distribution. These sample points are called sigma points and are symmetrically distributed around the mean. To be specific, $2n+1$ sigma points $X_{t-1|t-1}$ are selected according to:

$$X_{l,t-1|t-1} = \begin{cases} \hat{X}_{t-1|t-1} & l = 0 \\ \hat{X}_{t-1|t-1} - \sigma^l_{t-1} & l = 1, \ldots, n \\ \hat{X}_{t-1|t-1} + \sigma^l_{t-1} & l = n+1, \ldots, 2n \end{cases} \tag{4}$$

Then, each sigma point will be propagated through the system model, i.e., apply (2) to $X_{t-1|t-1}$ to get $X_{t|t-1}$. Next, the mean and covariance of the transformed points are used to calculate the new state estimation $\hat{X}_{t|t-1}$. Measurement $Y_{t|t-1}$ is calculated by applying (3) to $X_{t|t-1}$ and then is used to update the state estimation $\hat{X}_{t|t-1}$ to get $\hat{X}_{t|t}$, which is the state estimation at time t given observations up to and including at time t. Here, we assume that the state update is linear with Gaussian noise. Algorithm 1 illustrates the basic procedures. Details of UKF can be found in [15].

C. Granger Causality Test

Granger causality test is utilized to check the causal relationship between policy stringency and reproduction number. Here, we borrow the notion of "stringency index" from [2] (further explained in section III-A), which is an index that quantitatively reflects the strictness of containment and closure policies. A higher value means a stricter policy and vice versa. Granger causality test is a statistical hypothesis test for investigating the ability of one time series to forecast

Algorithm 1 Unscented Kalman Filter with SEIR Model

Input: SEIR model, measurement function, time series of total cases Y

Output: Estimated state $X = [S,\ E,\ I,\ R,\ \beta,\ \gamma]$

Let L be the length of measurement Y
for $t = 1 : L$ **do**
  Select $2n + 1$ sigma points $X_{t-1|t-1}$ according to (4)
  Compute $X_{t|t-1}$ by applying SEIR model in (2) to $X_{t-1|t-1}$
  Compute the predicted state $\hat{X}_{t|t-1}$ (and the error covariance matrix): $\hat{X}_{t|t-1} = \frac{1}{2n+1}\sum_{l=0}^{2n} X_{l,t|t-1}$
  Compute $Y_{t|t-1}$ by applying (3) to $X_{t|t-1}$
  Compute the predicted observation $\hat{Y}_{t|t-1}$: $\hat{Y}_{t|t-1} = \frac{1}{2n+1}\sum_{l=0}^{2n} Y_{l,t|t-1}$
  Compute the residual $e_t = Y_t - \hat{Y}_{t|t-1}$
  Update the Kalman gain matrix K_t
  Update the estimate of the state vector (and the error covariance matrix): $\hat{X}_{t|t} = \hat{X}_{t|t-1} + K_t e_t$ i.e., state estimation at time t given observations up to and including at time t
end for
return Estimated state $X = [S,\ E,\ I,\ R,\ \beta,\ \gamma]$

another, which is frequently used in the economics, finance, and medical fields [16]. Given two sets of time-series data x and y, we say x Granger-causes y if the past information of x could help forecast the future of y, over and above previous y information. Then, there is "information flow" from x to y [18]. Mathematically, we first define the univariate autoregressive model (Model1):

$$y_t = \sum_{k=1}^{K} \gamma_k y_{t-k} + e^t \tag{5}$$

Then, we define the bivariate autoregressive model (Model2):

$$y_t = \sum_{k=1}^{K} \gamma_k y_{t-k} + \sum_{k=1}^{K} \beta_k x_{t-k} + \epsilon_t \tag{6}$$

where y_t is the reproduction number, and x_t is the stringency index at time t and k is the number of lags. e^t and ϵ_t are white noises with zero mean and variances σ^2_{Model1} and σ^2_{Model2} respectively. The Granger causality is calculated as $log(\sigma^2_{Model1}/\sigma^2_{Model2})$. Based on (6), the null hypothesis is defined as H_0: β_1 = ... = β_k = 0. If H_0 is true, stringency index does not Granger-cause reproduction number [19].

We first check the "information flow" from stringency index to reproduction number, then test in the other direction. The procedures are as follows:

1) Assuming null hypothesis (H_0) is true.
2) Computing the parameter F test to access the statistical significance of Granger causality.
3) Comparing p-value to critical value 0.05.

If p-value is greater than 0.05, the null hypothesis is rejected and vice versa.

TABLE I
R^2 SCORE OF TWO DIFFERENT APPROACHES

Country	EKF with SEIR	UKF with SEIR
Italy	0.7401	**0.8180**
Turkey	0.9373	**0.9511**
United States	0.6995	**0.7530**
United Kingdom	0.5016	**0.8903**

D. Change Point Detection

If a country's stringency index Granger-causes the reproduction number, we will go further to detect the change points of stringency index and reproduction number estimated by UKF. The classical sequential approach, *Binary Segmentation* [20], is utilized to find the change points, as it does not require the number of change points in advance and is easy to implement. The first change point is detected in the complete input signal, then the series is split around this change point, and then the operation is repeated on the two resulting sub-signals. After detecting the change points, we are able to investigate the delay for the change of stringency index actually taken into effect. We define the delay T (days) as follows:

$$T = RN_j - SI_i \quad \text{s.t. } SI_i \leq RN_j < SI_{i+1} \tag{7}$$

where SI_i denotes the date of the i-th stringency index change point and RN_j denotes the date of the first reproduction number change point after SI_i. We assume that the delay T must be shorter than the time between two consecutive stringency index change points. Definition (7) is illustrated in the zoomed-in picture in Fig. 4.

III. Experiments and Results

A. Datasets and Preprocessing

The data of Italy, Turkey, United States and United Kingdom, for UKF estimation, is from [21]. We use the "total cases" column as the input data in the simulation. In order to evaluate the effectiveness of UKF estimation, the "reproduction number" column is taken as ground truth values. Furthermore, stringency index is obtained from [22]. In this dataset, each containment and closure policy is assigned a numerical value according to their stringency at each day and together forms the stringency index[1]. Since Granger causality test requires the two input time-series to be stationary, we first calculate the natural logarithm and take the forward difference on both stringency index and reproduction number. Then, augmented Dickey–Fuller test (ADF) [23] is conducted to make sure that both preprocessed series are stationary [24].

B. Estimation Results by Unscented Kalman Filter

Fig. 3 compares the UKF estimated reproduction number from April 19 to October 28, March 23 to December 18, April 04 to December 18, March 25 to December 18, with the ground truth value and a baseline method using EKF for

[1]Detailed information about stringency index calculation can be found at https://www.bsg.ox.ac.uk/research/research-projects/coronavirus-government-response-tracker

TABLE II
RESULTS OF GRANGER CAUSALITY TEST

Country	Direction[a]	P-value
Turkey	A to B	0.4149
	B to A	0.6458
United Kingdom	A to B	0.6457
	B to A	0.1642
United States	A to B	**0.0001**
	B to A	0.0918
Italy	A to B	**0.0217**
	B to A	0.1816

[a]A: Stringency Index B: Reproduction Number.

Turkey, United Kingdom, United States, and Italy respectively. Table I shows the performance evaluation of two approaches in terms of R^2 score. Although UKF and EKF are both capable of capturing the general trend of ground truth value, according to R^2 score, UKF (shown in bold) outperforms EKF by 0.0138, 0.3887, 0.0535, and 0.0779 for the aforementioned four countries respectively. Notably, the results of UKF estimations for Turkey and United Kingdom stand out with better R^2 score apparently, but the estimations of the other two countries are both fluctuating around the ground truth values. This phenomenon could be explained by the collection of data. For Italy, there are some missing data for particular dates, and in the case of United States, due to the time it takes to report testing information, the data might not represent the most current counts for the most recent three days. These factors may lead to the inconsistency between UKF estimation and the ground truth value [21].

C. Results of Granger Causality Test

Table II shows the results obtained by the Granger causality test. P-value in bold indicates pass of Granger causality test, meaning one of the two time-series Granger-causes the other one. It can be observed that in United States and Italy, stringency index Granger-causes reproduction number. In United Kingdom and Turkey, however, stringency index does not Granger-cause reproduction number, suggesting that containment and closure policies taken by the British and Turkish government seem to have little influence on the trend of COVID-19 pandemic.

D. Results of Change Point Detection

For the two countries showing Granger causality, change point detection algorithm is used to find the dates on which stringency index and reproduction number undergo significant change respectively (shown in Fig. 4). We observe that when containment and closure policy stringency changes, there exists some delay in its corresponding effect on the pandemic spread, possibly due to the slow reaction of the society. Since a lower value of stringency index suggests a looser policy, an inappropriate policy stringency change may result in significant growth of reproduction number. From the perspective of pandemic control, an effective policy change should lead to a decreasing or stable trend of the reproduction number.

For United States, the decrease in stringency index on June 14 and September 10 both resulted in the rise in reproduction number. Especially, the inappropriate stringency index change on September 10 led to a second increase in the reproduction number on October 7. Nonetheless, the decline in stringency index on June 19 did have positive effect on the control of pandemic, which was revealed by the decrease in reproduction number with 13-day delay. And after October 12, the changes of stringency index had minimal effect since no change point of reproduction number was detected. Overall, the delay is around 3 to 13 days.

For Italy, the changes of stringency index from June 13 to October 21 had negative impact on controlling the pandemic, especially the relaxation of stringency on September 13 led to dramatically increase in reproduction number with 17-day delay. In order to control the spreading, stricter policies were implemented on October 21 and November 5 and took into effect on October 31 and November 14 with 9 and 10-day delay. Overall, the delay is around 3 to 17 days.

IV. CONCLUSION

In this paper, we introduce a novel framework to track the spread of COVID-19 pandemic and evaluate the causal effect of containment and closure policy stringency based on the estimated dynamics. Substantial experiments are conducted on four countries include Italy, United Kingdom, United States, and Turkey. By leveraging unscented Kalman filter, we show that the estimated reproduction number is well-aligned with the ground truth value in terms of R^2 score. Next, containment and closure policy stringency is proved to Granger-cause reproduction number (R_0) in the cases of Italy and United States. Experimental results of change point detection also show that there exists several days of delay for the change of policy stringency to take into effect on reproduction number. In the future, the potential of using UKF to forecast R_0 will be investigated.

V. ACKNOWLEDGMENTS

The authors would like to thank Dr. Sena Beliner, M.D. and Dr. Caner Baysan, M.D. for very valuable discussions on epidemiology and public health strategies. This research is funded by Natural Science Foundation of China 62001266.

REFERENCES

[1] A. Atkeson, "What will be the economic impact of covid-19 in the us? rough estimates of disease scenarios," National Bureau of Economic Research, Tech. Rep., 2020.

[2] T. Hale, A. Petherick, T. Phillips, and S. Webster, "Variation in government responses to covid-19," *Blavatnik school of government working paper*, vol. 31, pp. 2020–11, 2020.

[3] W. O. Kermack and A. G. McKendrick, "A contribution to the mathematical theory of epidemics," *Proceedings of the royal society of london. Series A, Containing papers of a mathematical and physical character*, vol. 115, no. 772, pp. 700–721, 1927.

[4] R. M. Anderson and R. M. May, *Infectious diseases of humans: dynamics and control*. Oxford university press, 1992.

[5] H. W. Hethcote, "The mathematics of infectious diseases," *SIAM review*, vol. 42, no. 4, pp. 599–653, 2000.

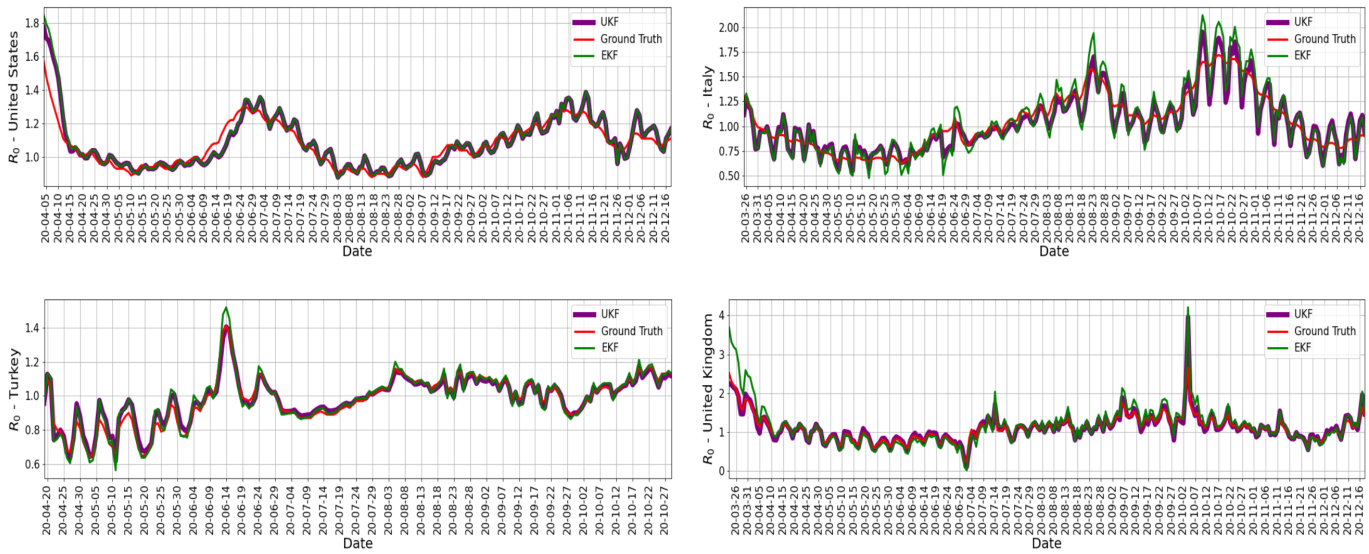

Fig. 3. Estimations of Reproduction Number

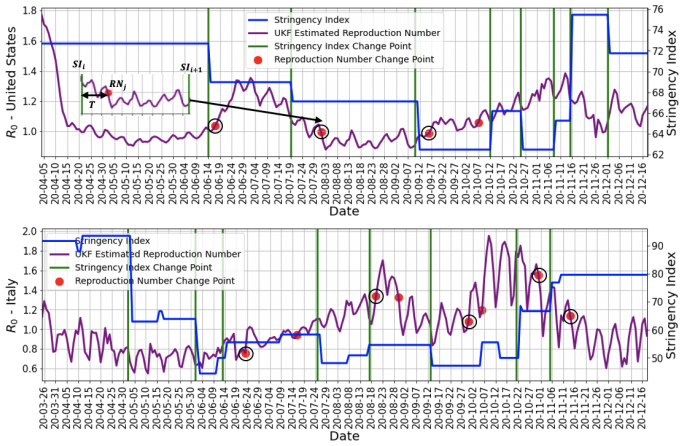

Fig. 4. Change Point Detection. Purple Line: Estimated Reproduction Number by UKF. Blue Line: Stringency Index. Vertical Green Line: Detected Stringency Index Change Point. Red Dot: Detected Reproduction Number Change Point. Black Circle: Delay Point corresponding to Stringency Index Change Point.

[6] E. L. Piccolomini and F. Zama, "Preliminary analysis of covid-19 spread in italy with an adaptive seird model," *arXiv preprint arXiv:2003.09909*, 2020.

[7] D. Khatua, A. De, S. Kar, E. Samanta, A. A. Seikh, and D. Guha, "A fuzzy dynamic optimal model for covid-19 epidemic in india based on granular differentiability," *Available at SSRN 3621640*, 2020.

[8] Q. Yang, C. Yi, A. Vajdi, L. W. Cohnstaedt, H. Wu, X. Guo, and C. M. Scoglio, "Short-term forecasts and long-term mitigation evaluations for the covid-19 epidemic in hubei province, china," *Infectious Disease Modelling*, vol. 5, pp. 563–574, 2020.

[9] A. Gomez-Exposito, J. A. Rosendo-Macias, and M. A. Gonzalez-Cagigal, "Monitoring and tracking the evolution of a viral epidemic through nonlinear kalman filtering: Application to the covid-19 case," *medRxiv*, 2020.

[10] W. Lyra, J.-D. do Nascimento Jr, J. Belkhiria, L. de Almeida, P. P. M. Chrispim, and I. de Andrade, "Covid-19 pandemics modeling with modified determinist seir, social distancing, and age stratification. the effect of vertical confinement and release in brazil," *Plos one*, vol. 15, no. 9, p. e0237627, 2020.

[11] A. Aravindakshan, J. Boehnke, E. Gholami, and A. Nayak, "Preparing for a future covid-19 wave: insights and limitations from a data-driven evaluation of non-pharmaceutical interventions in germany," *Scientific reports*, vol. 10, no. 1, pp. 1–14, 2020.

[12] N. G. Davies, A. J. Kucharski, R. M. Eggo, A. Gimma, W. J. Edmunds, T. Jombart, K. O'Reilly, A. Endo, J. Hellewell, E. S. Nightingale *et al.*, "Effects of non-pharmaceutical interventions on covid-19 cases, deaths, and demand for hospital services in the uk: a modelling study," *The Lancet Public Health*, vol. 5, no. 7, pp. e375–e385, 2020.

[13] N. Haug, L. Geyrhofer, A. Londei, E. Dervic, A. Desvars-Larrive, V. Loreto, B. Pinior, S. Thurner, and P. Klimek, "Ranking the effectiveness of worldwide covid-19 government interventions," *Nature human behaviour*, vol. 4, no. 12, pp. 1303–1312, 2020.

[14] J. M. Brauner, S. Mindermann, M. Sharma, D. Johnston, J. Salvatier, T. Gavenčiak, A. B. Stephenson, G. Leech, G. Altman, V. Mikulik *et al.*, "Inferring the effectiveness of government interventions against covid-19," *Science*, vol. 371, no. 6531, 2021.

[15] S. J. Julier and J. K. Uhlmann, "New extension of the kalman filter to nonlinear systems," in *Signal processing, sensor fusion, and target recognition VI*, vol. 3068. International Society for Optics and Photonics, 1997, pp. 182–193.

[16] C. W. Granger, "Investigating causal relations by econometric models and cross-spectral methods," *Econometrica: journal of the Econometric Society*, pp. 424–438, 1969.

[17] Q. Li, X. Guan, P. Wu, X. Wang, L. Zhou, Y. Tong, R. Ren, K. S. Leung, E. H. Lau, J. Y. Wong *et al.*, "Early transmission dynamics in wuhan, china, of novel coronavirus–infected pneumonia," *New England journal of medicine*, vol. 382, no. 13, pp. 1199–1207, 2020.

[18] A. K. Seth, A. B. Barrett, and L. Barnett, "Granger causality analysis in neuroscience and neuroimaging," *Journal of Neuroscience*, vol. 35, no. 8, pp. 3293–3297, 2015.

[19] E. Siggiridou and D. Kugiumtzis, "Granger causality in multivariate time series using a time-ordered restricted vector autoregressive model," *IEEE Transactions on Signal Processing*, vol. 64, no. 7, pp. 1759–1773, 2015.

[20] J. Bai, "Estimating multiple breaks one at a time," *Econometric theory*, pp. 315–352, 1997.

[21] H. R. Max Roser, "Coronavirus pandemic (covid-19)," *Our World in Data*, 2020, https://ourworldindata.org/coronavirus.

[22] T. Hale and S. Webster, "Oxford covid-19 government response tracker," 2020.

[23] D. A. Dickey and W. A. Fuller, "Likelihood ratio statistics for autoregressive time series with a unit root," *Econometrica: journal of the Econometric Society*, pp. 1057–1072, 1981.

[24] L.-C. Lee, P.-H. Lin, Y.-W. Chuang, and Y.-Y. Lee, "Research output and economic productivity: a granger causality test," *Scientometrics*, vol. 89, no. 2, pp. 465–478, 2011.